The Astrophysical Journal Letters, 881:L32 (4pp), 2019 August 20 https://doi.org/10.3847/2041-8213/ab3920

Type I Outbursts in Low-eccentricity Be/X-Ray Binaries

Alessia Franchini and Rebecca G. Martin
Department of Physics and Astronomy, University of Nevada, 4505 South Maryland Parkway, Las Vegas, NV 89154, USA; alessia.franchini@unlv.edu
Received 2019 July 1; revised 2019 July 25; accepted 2019 August 7; published 2019 August 20

Abstract

Type I outbursts in Be/X-ray binaries are usually associated with the eccentricity of the binary orbit. The neutron star accretes gas from the outer parts of the decretion disk around the Be star at each periastron passage. However, this mechanism cannot explain type I outbursts that have been observed in nearly circular orbit Be/X-ray binaries. With hydrodynamical simulations and analytic estimates we find that in a circular orbit binary, a nearly coplanar disk around the Be star can become eccentric. The extreme mass ratio of the binary leads to the presence of the 3:1 Lindblad resonance inside the Be star disk and this drives eccentricity growth. Therefore the neutron star can capture material each time it approaches the disk apastron, on a timescale up to a few percent longer than the orbital period. We have found a new application of this mechanism that is able to explain the observed type I outbursts in low-eccentricity Be/X-ray binaries.

Unified Astronomy Thesaurus concepts: Accretion (14); Circumstellar disks (235); X-ray binary stars (1811); Hydrodynamics (1963); Pulsars (1306); B(e) stars (2104)

1. Introduction

Be/X-ray binaries are composed typically of a Be star and a neutron star companion. The Be star is surrounded by a geometrically thin Keplerian decretion disk (Lee et al. 1991; Pringle 1991; Porter 1996; Cassinelli et al. 2002; Porter & Rivinius 2003) that is truncated by the tidal force exerted by the companion (Okazaki et al. 2002; Hayasaki & Okazaki 2004; Martin et al. 2011). These systems can be persistent sources of X-rays or they can be transient, meaning that they alternate quiescent states with outbursts. The outbursts are divided into two categories: type I and type II (or giant) depending on the duration and on the peak X-ray luminosity (Stella 1986; Negueruela 1998; Okazaki et al. 2002). Type I outbursts occur on the orbital period and are usually less bright ($L_X = 0.01-0.1\,L_{Edd}$) while type II last several orbital periods and are brighter ($L_X > 0.1\,L_{Edd}$).

The majority of the observed systems have eccentric orbits. This naturally explains the occurrence of type I outbursts when the neutron star passes through periastron and collects material from the outer parts of the Be star decretion disk (Negueruela & Okazaki 2001; Okazaki & Negueruela 2001). However, there are some examples of Be/X-ray binaries with nearly circular orbits that show type I outbursts (Pfahl et al. 2002; Reig 2007). For example, XTE J1948+32, which has an orbital eccentricity of $e = 0.03$ and an orbital period of 40.4 days (Raguzova & Popov 2005; Reig 2007; Reig & Nespoli 2013). GS 0834–430 has orbital eccentricity $e = 0.12$ and a 105.8 day orbital period and shows five type I outbursts reoccurring on a timescale of 107 days (Wilson et al. 1997; Townsend et al. 2011; Cheng et al. 2014). XTE J1543-568 has an orbital eccentricity $e < 0.03$ and a 75.6 day orbital period (Reig 2007; Reig & Nespoli 2013; Cheng et al. 2014). Finally, 2S 1553–542 has an orbital eccentricity $e < 0.09$ and an orbital period of 30.6 days (Reig 2007).

In this Letter, we focus on the mechanism that leads to type I outbursts in nearly circular Be/X-ray binaries. In Section 2 we describe the results of hydrodynamical simulations of a low-eccentricity Be/X-ray binary system. We find that the disk becomes eccentric and this leads to type I like outbursts when the neutron star is close to the disk apastron. In Section 3 we explain the disk eccentricity growth by the presence of the 3:1 Lindblad resonance within the disk (Lubow 1991a, 1991b, 1992). Previous studies suggested that this mechanism could not drive eccentricity growth in Be star disks since the disk may be truncated at the 3:1 resonance location (e.g., Okazaki & Negueruela 2001). However, we show that the disk is able to extend farther out than the 3:1 resonance. We draw our conclusions in Section 4.

2. Hydrodynamical Simulations

We use the smoothed particle hydrodynamics (SPH) code PHANTOM (Lodato & Price 2010; Price et al. 2018) to model a binary system composed of a Be star surrounded by a coplanar accretion disk and a companion neutron star on a circular orbit. Disks in binary systems have been extensively studied with PHANTOM (e.g., Nixon 2012; Nixon & Lubow 2015; Franchini et al. 2019). We perform SPH simulations with $N = 5 \times 10^5$ particles. The resolution of the simulation depends on N, the viscosity parameter α, and the disk scale height H. The Shakura & Sunyaev (1973) viscosity parameter is modeled by adapting artificial viscosity according to the approach of Lodato & Price (2010). With this choice of parameters the disk is initially resolved with a shell-averaged smoothing length per scale height of $\langle h \rangle / H = 0.628$, and this does not change much over the simulation.

The binary components are modeled as sink particles with masses $M_* = 18\,M_\odot$ and $M_{NS} = 1.4\,M_\odot$. The binary mass ratio is therefore $q = M_{NS}/M_\star = 0.078$. We choose a binary separation of $a = 95\,R_\odot$, corresponding to an orbital period of $P_b = 24.3$ days. The orbital period is $P_b = 2\pi/\Omega_b$, where $\Omega_b = \sqrt{G(M_\star + M_{NS})/a^3}$. We discuss how this choice of binary orbital period affects our results in Section 3.1. The accretion radii of the sink particles are chosen to be $R_{acc,\star} = 8\,R_\odot$ and $R_{acc,NS} = 0.5\,R_\odot$ for the Be star and the neutron star, respectively. Particles inside these radii are accreted onto the respective sink particle. The accretion disk around the Be star extends from $R_{in} = 8\,R_\odot$ to an outer radius $R_{out} = 50\,R_\odot$ initially and has a total initial mass of $M_d = 1 \times 10^{-8} M_\odot$. We take the viscosity parameter to be $\alpha = 0.3$, which is typical for fully ionized accretion disks (King et al. 2007; Rímulo et al. 2018;

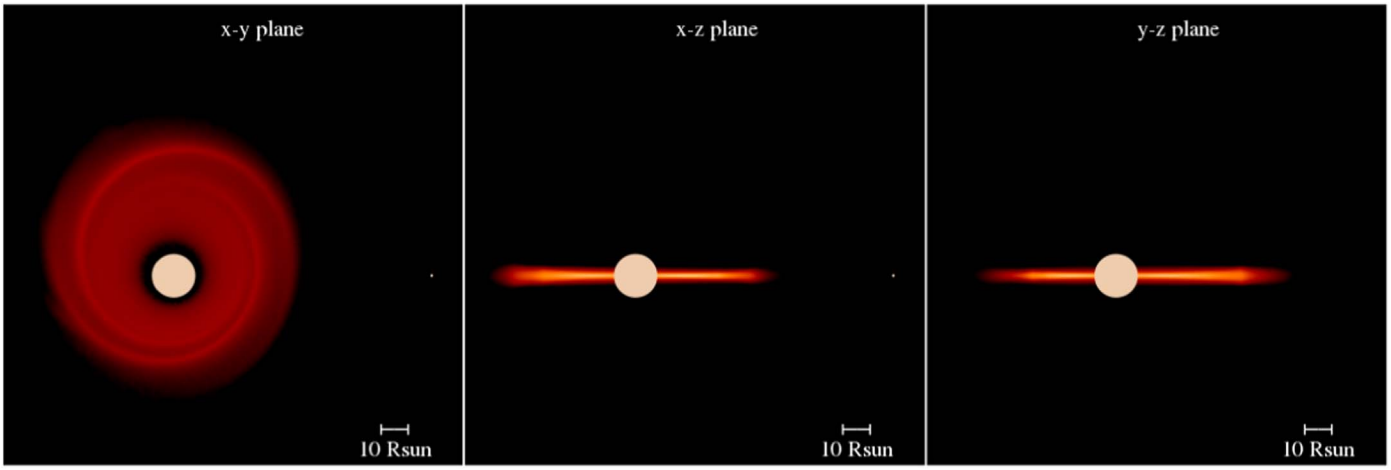

Figure 1. Column density of the Be star accretion disk from the SPH simulation at time $t = 30\,P_{\rm b}$. The Be star is represented by the large white circle, while the small white circle represents the companion neutron star. The size of the circle denotes the accretion radius of the sink. The left panel shows the view looking down on the x–y binary orbital plane, while the middle and right panels show the view in the x–z and y–z planes, respectively. The disk is initially circular and coplanar to the binary orbital plane. The Be star disk becomes eccentric due to the presence of the 3:1 resonance within the disk.

Martin et al. 2019). We assume a globally isothermal equation of state for the gas with $H/R = 0.01$ at the disk inner edge. This leads to $H/R = 0.025$ at the initial disk outer radius. The initial surface density profile is $\Sigma \propto R^{-p}$ with $p = 1$. The neutron star does not have an accretion disk at the beginning of the simulation. The Be star accretion disk initially expands slightly, reaching the tidal truncation radius (Artymowicz & Lubow 1994; Paczynski 1977).

Figure 1 shows the disk column density at a time of $30\,P_{\rm b}$ in our simulation. The left, middle, and right panels show the view in the x–y, x–z, and y–z planes, respectively. We can clearly see that the disk remains coplanar to the binary orbital plane but becomes eccentric.

Figure 2 shows the eccentricity and argument of periapsis angle evolution of the Be star disk. Both quantities are measured from our simulation through a density-weighted average over the radial extent of the disk. The eccentricity vector of the disk is precessing around the Be star on a timescale of about $40\,P_{\rm b}$, while the magnitude of the eccentricity grows. Figure 3 shows the disk surface density (top panel) and eccentricity (bottom panel) profile at five different times $t = 0$, 10, 20, 30, $40\,P_{\rm b}$. Most of the material that is lost from the disk is accreted on to the Be star. A small fraction is transferred on to the neutron star and some forms circumbinary material (Franchini et al. 2019). The bottom panel of Figure 3 shows that the eccentricity growth begins in the outer parts of the disk and is communicated through pressure in the disk to the inner parts.

Figure 4 shows the accretion rate (top panel) and the total mass accreted (bottom panel) onto the neutron star as a function of time. We see the occurrence of type I outbursts in the accretion rate on a timescale of about $1.02\,P_{\rm b}$ starting after the first few binary orbits when the disk eccentricity starts to grow and the neutron star is able to capture material when it passes close to the disk apastron.

We can estimate the X-ray luminosity reached during the outbursts to be $L_{\rm X} \approx 0.09\,L_{\rm Edd}$ (see Equation (3) in Martin et al. 2014), which is the typical value observed in type I outbursts. Therefore, for the accretion rate onto the neutron star

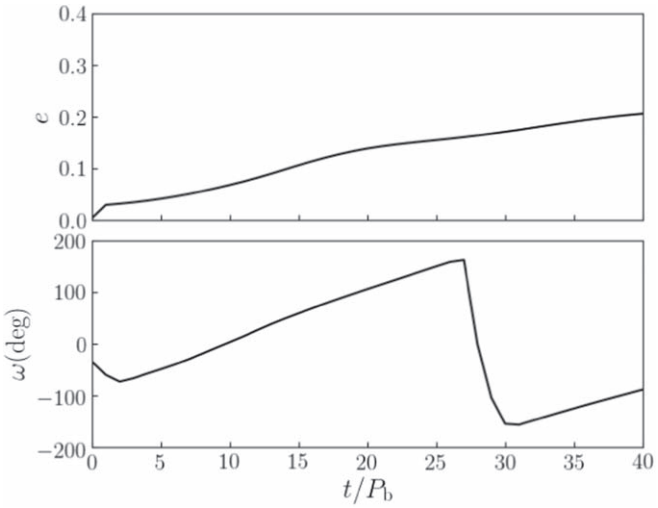

Figure 2. Density-weighted average disk eccentricity (top panel) and argument of periapsis (bottom panel) evolution of the disk around the Be star. The Be star disk starts with zero eccentricity and is coplanar to the binary plane.

to produce the observed X-ray luminosity we require the disk mass to be $M_{\rm d} \lesssim 10^{-8}\,M_{\odot}$.

2.1. Effect of Disk Inclination

We also investigated, through hydrodynamical simulations, the effect of the initial Be star disk inclination relative to the binary orbital plane on the disk eccentricity growth. We found that the eccentricity growth is not sufficient to induce outbursts if the inclination angle is above about 20°. Therefore, the mechanism presented here would not drive type I outbursts in sources with large Be star spin misalignments with respect to the binary orbital plane.

While we do not have observational evidence of the alignment of the disk, we expect the disk in a low-eccentricity system to be close to coplanar to the binary orbit. Prior to the formation of the neutron star, we expect that the spin of the Be star will be aligned to a circular binary orbit. Supernova explosions may be asymmetric leading to a kick on the newly

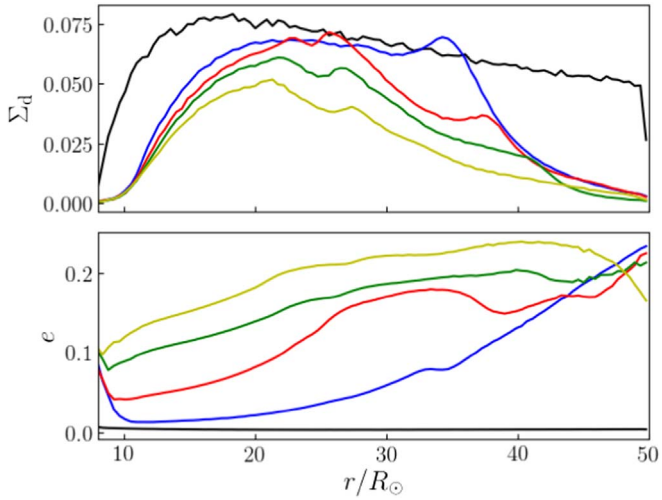

Figure 3. Surface density profile (top panel) and eccentricity (bottom panel) of the Be star disk as a function of radius. The lines represent the quantities at time $t = 0$ (black), $t = 10\,P_b$ (blue), $t = 20\,P_b$ (red), $t = 30\,P_b$ (green), and $t = 40\,P_b$ (yellow).

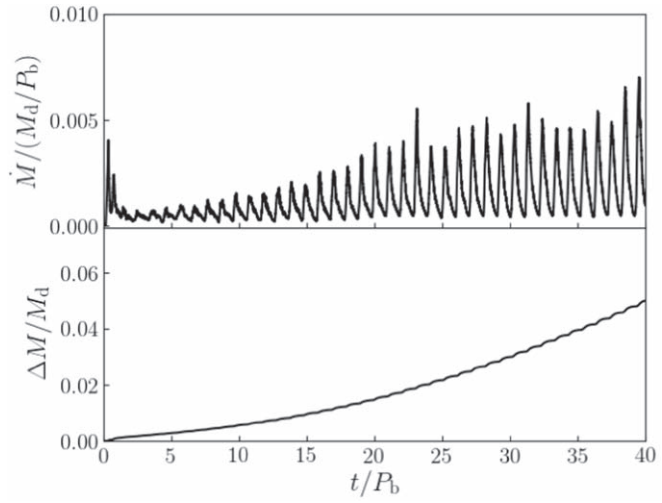

Figure 4. Top panel: accretion rate onto the neutron star (at an accretion radius of $0.5\,R_\odot$). Bottom panel: total accreted mass onto the neutron star in units of the initial disk mass $M_d = 10^{-8}\,M_\odot$ vs. time in units of the binary orbital period.

formed neutron star (Sutantyo 1978). This kick leads to an eccentric and inclined orbit (Brandt & Podsiadlowski 1995; Martin et al. 2009). Since the Be star binaries we consider in this work have low eccentricity, we also expect that they will have low misalignment angles (e.g., Podsiadlowski et al. 2004).

3. Eccentricity Growth in the Be Star Disk

The radius of the 3:1 resonance is

$$R_{\rm res} = 3^{-2/3}(1+q)^{-1/3}a \tag{1}$$

(e.g., Goodchild & Ogilvie 2006). For our parameters, this is at a radius of $44.5\,R_\odot$. This leads to eccentricity growth within the disk at a rate

$$\lambda \simeq 2.1\,q^2\,\Omega_b\,\frac{R_{\rm res}}{W} \tag{2}$$

(Lubow 1992), where W is the disk radial extent. The growth rate predicted for our set of parameters is $\lambda \simeq 0.002\,P_b^{-1}$. The rate at which the Be star disk eccentricity grows as shown in Figure 2 is about 0.2 in 40 binary orbits, or $\lambda = 0.005\,P_b^{-1}$, higher than the theoretical prediction from Equation (2). This discrepancy is likely due to the fact that Equation (2) does not depend on the gas sound speed and viscosity. Higher viscosities and smaller disk aspect ratios both lead to faster disk eccentricity growth (e.g., Kley et al. 2008).

The disk can become eccentric enough to fill the Be star Roche lobe and overflow onto the neutron star forming a misaligned and initially eccentric accretion disk (Martin et al. 2014; Franchini et al. 2019). The minimum eccentricity required for the disk to fill the Be star Roche lobe in this configuration can be obtained comparing the radius of the disk apastron with the Roche-lobe radius (Eggleton 1983) and for our choice of parameters is $e_{\rm min} = 0.14$ assuming an outer disk radius of $50\,R_\odot$. The accretion rate in Figure 4 shows that the outbursts become significant after about $10\,P_b$ when the disk outer edge reaches an eccentricity of 0.2 (see the blue line in the bottom panel of Figure 3).

The eccentric disk precesses in a prograde direction with period P_p, which is much longer than the orbital period. Therefore, the companion neutron star reaches the line of apsides on a period slightly longer than the orbital period of the binary. The outburst period, $P_{\rm burst}$, is known as the apsidal superhump period in cataclysmic variables (e.g., Whitehurst 1988; Hirose & Osaki 1990; Whitehurst & King 1991) and it is related to the orbital period with

$$P_{\rm burst} \simeq P_b\left(1+\frac{P_b}{P_p}\right) \tag{3}$$

(e.g., Murray 1998) if the precession period is long compared to the binary orbital period. The precession period for the disk can be approximated with

$$P_p = \frac{2\pi}{\omega_{\rm dyn}}, \tag{4}$$

where the dynamical component provides a prograde precession with frequency given by

$$\omega_{\rm dyn} = \frac{1}{4r^2}\frac{d}{dr}\left(r^2\frac{db_{1/2}^{(0)}}{dr}\right)\frac{q}{\sqrt{1+q}}\Omega_b, \tag{5}$$

where the radius is scaled to the binary orbital semimajor axis, $r = R/a$, and $b_{1/2}^{(0)}$ is the Laplace coefficient from celestial mechanics calculations (Murray 2000). For a mass ratio $q = 0.078$ and $r = 0.47$ we find $\omega_{\rm dyn}/\Omega_b = 0.029$, and this corresponds to a precession period $P_p = 34.8\,P_b$. The corresponding outburst period is $P_{\rm burst} = 1.028\,P_b$.

This estimate is an upper limit to the outburst period since the effects of pressure introduce a retrograde component (Lubow 1992; Murray 1998, 2000; Kley et al. 2008). The timescale between outbursts estimated from the simulation (see Figure 4) is indeed slightly shorter than the one predicted here without considering pressure effects. For a sufficiently large disk aspect ratio, the precession may even become retrograde (e.g., Kley et al. 2008). The precession rate is insensitive to the disk viscosity (unless the viscosity is very small); therefore, accurate measurements of the type I outburst period in low-eccentricity X-ray binaries may also help to constrain the observed value for H/R.

3.1. Effect of Orbital Period

The simulation we presented in Section 2 is for a specific orbital period, but the mechanism can operate for a wide range of parameters provided that the disk is large enough to reach the 3:1 resonance location and the disk aspect ratio there is small enough.

For longer-period Be/X-ray binaries the possibility of having type I outbursts in low-eccentricity systems depends on the Be star disk aspect ratio at the resonance radius. The strength of the 3:1 resonance scales with $(H/R)^{-2}$ (Goodchild & Ogilvie 2006). Therefore, the larger the disk aspect ratio at the resonance radius, the weaker the resonance. For a fixed binary mass ratio, the resonance location and the tidal truncation radius both scale with semimajor axis. If the disk aspect ratio at the resonance radius is too large, the source is unlikely to undergo type I outbursts. Instead, its behavior would be similar to a persistent X-ray emitter rather than a transient. Thus, this mechanism is more likely to operate for smaller orbital period binaries ($P_{\rm b} \lesssim 150$ days), assuming that the disks are flared.

The inferred period for type I outbursts taking into account the apsidal precession of the disk might be able to explain also the difference between the binary orbital period of 105.8 ± 0.4 days and the observed outburst timescale of 107 days for the source GS 0834–430 (Wilson et al. 1997). These outbursts reoccur on a timescale of 1.007–1.015 $P_{\rm b}$.

4. Conclusions

We have investigated type I outbursts in nearly circular, relatively short period Be/X-ray binaries. The presence of the 3:1 Lindblad resonance within the Be star disk leads to significant eccentricity growth. We found a new application of this mechanism to explain this type of outburst if the Be star decretion disk is close to coplanar with the binary orbital plane. The neutron star is able to capture material every time it passes the disk apastron, thus producing type I outbursts. This mechanism for driving type I outbursts in a circular orbit binary relies on two system properties. First, the disk must be large enough to reach the location of the 3:1 Lindblad resonance given in Equation (1), and this is valid for binary mass ratios $q \lesssim 0.33$ (Frank et al. 2002). Second, the disk aspect ratio must be small enough at the resonance radius in order for the 3:1 Lindblad resonance to be able to drive eccentricity growth in the disk. This means that the mechanism is more likely to operate for shorter orbital period binaries, if the disks are flared.

We thank Daniel Price for providing the PHANTOM code for SPH simulations and acknowledge the use of SPLASH (Price & Monaghan 2007) for the rendering of the figures. We acknowledge support from NASA through grant NNX17AB96G. Computer support was provided by UNLV's National Supercomputing Center.

ORCID iDs

Alessia Franchini https://orcid.org/0000-0002-8400-0969
Rebecca G. Martin https://orcid.org/0000-0003-2401-7168

References

Artymowicz, P., & Lubow, S. H. 1994, ApJ, 421, 651
Brandt, N., & Podsiadlowski, P. 1995, MNRAS, 274, 461
Cassinelli, J. P., Brown, J. C., Maheswaran, M., Miller, N. A., & Telfer, D. C. 2002, ApJ, 578, 951
Cheng, Z. Q., Shao, Y., & Li, X. D. 2014, ApJ, 786, 128
Eggleton, P. P. 1983, ApJ, 268, 368
Franchini, A., Martin, R. G., & Lubow, S. H. 2019, MNRAS, 485, 315
Frank, J., King, A., & Raine, D. J. 2002, Accretion Power in Astrophysics (3rd ed.; Cambridge: Cambridge Univ. Press)
Goodchild, S., & Ogilvie, G. 2006, MNRAS, 368, 1123
Hayasaki, K., & Okazaki, A. T. 2004, MNRAS, 350, 971
Hirose, M., & Osaki, Y. 1990, PASJ, 42, 135
King, A. R., Pringle, J. E., & Livio, M. 2007, MNRAS, 376, 1740
Kley, W., Papaloizou, J. C. B., & Ogilvie, G. I. 2008, A&A, 487, 671
Lee, U., Osaki, Y., & Saio, H. 1991, MNRAS, 250, 432
Lodato, G., & Price, D. J. 2010, MNRAS, 405, 1212
Lubow, S. H. 1991a, ApJ, 381, 259
Lubow, S. H. 1991b, ApJ, 381, 268
Lubow, S. H. 1992, ApJ, 401, 317
Martin, R. G., Nixon, C., Armitage, P. J., Lubow, S. H., & Price, D. J. 2014, ApJL, 790, L34
Martin, R. G., Nixon, C. J., Pringle, J. E., & Livio, M. 2019, NewA, 70, 7
Martin, R. G., Pringle, J. E., Tout, C. A., & Lubow, S. H. 2011, MNRAS, 416, 2827
Martin, R. G., Tout, C. A., & Pringle, J. E. 2009, MNRAS, 397, 1563
Murray, J. R. 1998, MNRAS, 297, 323
Murray, J. R. 2000, MNRAS, 314, L1
Negueruela, I. 1998, A&A, 338, 505
Negueruela, I., & Okazaki, A. T. 2001, A&A, 369, 108
Nixon, C., & Lubow, S. H. 2015, MNRAS, 448, 3472
Nixon, C. J. 2012, MNRAS, 423, 2597
Okazaki, A. T., Bate, M. R., Ogilvie, G. I., & Pringle, J. E. 2002, MNRAS, 337, 967
Okazaki, A. T., & Negueruela, I. 2001, A&A, 377, 161
Paczynski, B. 1977, ApJ, 216, 822
Pfahl, E., Rappaport, S., Podsiadlowski, P., & Spruit, H. 2002, ApJ, 574, 364
Podsiadlowski, P., Langer, N., Poelarends, A. J. T., et al. 2004, ApJ, 612, 1044
Porter, J. M. 1996, MNRAS, 280, L31
Porter, J. M., & Rivinius, T. 2003, PASP, 115, 1153
Price, D. J., & Monaghan, J. J. 2007, MNRAS, 374, 1347
Price, D. J., Wurster, J., Nixon, C., et al. 2018, PASA, 35, e031
Pringle, J. E. 1991, MNRAS, 248, 754
Raguzova, N. V., & Popov, S. B. 2005, A&AT, 24, 151
Reig, P. 2007, MNRAS, 377, 867
Reig, P., & Nespoli, E. 2013, A&A, 551, A1
Rímulo, L. R., Carciofi, A. C., Vieira, R. G., et al. 2018, MNRAS, 476, 3555
Shakura, N. I., & Sunyaev, R. A. 1973, A&A, 24, 337
Stella, L. 1986, in Proc. Plasma Penetration into Magnetospheres, ed. N. Kylafis, J. Papamastorakis, & J. Ventura (Athina: Crete Univ. Press), 199
Sutantyo, W. 1978, Ap&SS, 54, 479
Townsend, L. J., Coe, M. J., Corbet, R. H. D., & Hill, A. B. 2011, MNRAS, 416, 1556
Whitehurst, R. 1988, MNRAS, 232, 35
Whitehurst, R., & King, A. 1991, MNRAS, 249, 25
Wilson, C. A., Finger, M. H., Harmon, B. A., et al. 1997, ApJ, 479, 388